

Jahn-Teller distortions and the magnetic order in the perovskite manganites

Krzysztof Rościszewski¹ and Andrzej M. Oleś^{1,2}

¹ Marian Smoluchowski Institute of Physics, Jagellonian University, Reymonta 4, PL-30059 Kraków, Poland

² Max-Planck-Institut für Festkörperforschung, Heisenbergstrasse 1, D-70569 Stuttgart, Germany

E-mail: roscis@th.if.uj.edu.pl; a.m.oles@fkf.mpg.de

Abstract. We introduce an effective model for e_g electrons to describe three-dimensional perovskite ($\text{La}_{1-x}\text{Sr}_x\text{MnO}_3$ and $\text{La}_{1-x}\text{Ca}_x\text{MnO}_3$) manganites and study the magnetic and orbital order on $4 \times 4 \times 4$ cluster using correlated wave functions. The model includes the kinetic energy, and on-site Coulomb interactions for e_g electrons, antiferromagnetic superexchange interaction between $S = 3/2$ core spins, and the coupling between e_g electrons and Jahn-Teller modes. The model reproduces the experimentally observed magnetic order: (i) *A*-type antiferromagnetic phase in the undoped insulator LaMnO_3 , with alternating e_g orbitals and with small Jahn-Teller distortions, changing to a conducting phase at 32 GPa pressure, and (ii) ferromagnetic order in one-eighth doped $\text{La}_{7/8}\text{Sr}_{1/8}\text{MnO}_3$ and in quarter doped $\text{La}_{3/4}\text{Sr}_{1/4}\text{MnO}_3$ compounds. For half-doped $\text{La}_{1/2}\text{Ca}_{1/2}\text{MnO}_3$ one finds a competition between a ferromagnetic conductor and the CE insulating phase; the latter is stabilized by the Jahn-Teller coupling being twice larger than for the strontium-doped compound. Altogether, there is a subtle balance between all Hamiltonian parameters and the phase diagram is quite sensitive to the precise values they take.

PACS numbers: 75.47.Gk, 75.10.Lp, 75.25.Dk, 63.20.Pw

Published in: J. Phys.: Condensed Matter **22**, 425601 (2010).

1. Introduction

Much effort was put into understanding what is going on in doped perovskite manganite oxides both on theoretical [1–13] and experimental [14–26] side. Early expectations that simple physical mechanisms, such as involving for example only Jahn-Teller (JT) interactions and Hund’s exchange but without Coulomb interaction, or pure electronic Coulomb interactions while neglecting Hund’s exchange, could explain the phase diagram and the phase transitions observed situations in the manganites were not confirmed [1,8]. Also relatively early it was realized that the core t_{2g} electrons, even if dynamically passive, play an essential role for the stability of magnetic and orbital order [4,11]. Altogether, the evidence has accumulated that there is a delicate balance between several competing physical mechanisms which lead to rather complex phase diagram of the perovskite manganites [1,11,13].

Investigation of doped manganites is challenging as the Jahn-Teller distortions may lead to the charge order which will also favour particular orbital order [1,27]. To make the complex situation in doped manganites tractable in the theory, several theoretical papers were focused in past on single-layer and double-layer manganites as the description of quasi two-dimensional (2D) systems was simpler than the one necessary for three-dimensional (3D) doped perovskite manganites (see for example [11] and the references therein). Realistic 3D systems were more difficult to tackle at least on a better basis than simple mean-field type approaches. Due to strong local correlations, however, such approaches were not quite appropriate to provide a better insight into the competition between different possible physical mechanisms present in these strongly correlated electron systems. The present paper is one attempt (among the others) to fill up this gap.

Similar to model studies [5,11], it has been also recognized in the electronic structure calculations performed within the local density approximation (LDA) that the local interactions are important and one has to use either LDA+ U or LDA+DMFT [12,28], i.e., take into account also the dynamical aspects in the dynamical mean field theory. These calculations confirmed the earlier point of view [5,29] that electron-electron interactions and the Jahn-Teller terms support each other and both are necessary to reproduce the observed orbital order in the undoped compound. In particular, by the studying the effect of pressure it was concluded that LaMnO_3 is not a Mott-Hubbard insulator, but rather a Jahn-Teller insulator, however, it has been recognized that the correlations play also an important role [28].

The paper is organised as follows. First, we introduce (in section 2) a *realistic* model for e_g electrons in the perovskite manganites which includes the electron Coulomb interactions, the coupling between e_g electrons with $s = 1/2$ spins and t_{2g} core $S = 3/2$ spins, superexchange interaction, and the interactions of e_g electrons with local distortions due to the Jahn-Teller terms (section 2.1). In this section we also present the method to determine approximate ground states using a $4 \times 4 \times 4$ cluster. We treat electron correlation effects in the ground state beyond the Hartree-Fock

(HF) approximation using the so-called local approach (section 2.2). The numerical results are presented and analysed in section 3. Here we address a question which values of the parameters of the effective Hamiltonian are appropriate to account for the experimentally observed situation and present results obtained for the undoped LaMnO_3 , and for $\text{La}_{1-x}\text{Sr}_x\text{MnO}_3$ at doping levels $x = 0.125, 0.25$ and 0.50 . Finally, section 4 contains a short summary of the paper and general conclusions.

2. The model and calculation method

2.1. The model for e_g electrons

We study strongly correlated electrons in undoped and doped 3D perovskite manganites $\text{La}_{1-x}\text{Sr}_x\text{MnO}_3$ (or $\text{La}_{1-x}\text{Ca}_x\text{MnO}_3$) using effective model describing only Mn sites renormalised by surrounding oxygens. At each site we consider Wannier orbitals of the e_g character composed out of manganese and oxygen orbitals [12]. One of them is filled at Mn^{3+} ions, and both are empty at Mn^{4+} ions in a doped system. In both cases the t_{2g} orbitals on Mn ions are occupied by three "core" electrons with total spin $S = 3/2$ (treated as frozen and classical). Thus the active electrons here are only e_g electrons. We investigate the system by using a model Hamiltonian

$$\mathcal{H} = H_{\text{kin}} + H_{\text{int}} + H_{\text{spin}} + H_{\text{JT}} \quad (1)$$

which consists of the kinetic energy, the on-site Coulomb interactions, spin interactions, and the Jahn-Teller term. This model and/or the essential parts of it, were studied earlier by several groups, see refs. [1, 7, 8, 11–13, 19, 30–33].

The kinetic part H_{kin} is expressed using a local e_g orbital basis at each site, which reads in short notation,

$$|z\rangle \equiv (3z^2 - r^2)/\sqrt{6}, \quad |x\rangle \equiv (x^2 - y^2)/\sqrt{2}. \quad (2)$$

Using this local e_g orbital basis at each site one finds anisotropic phase-dependent hopping [8, 11, 12]

$$\begin{aligned} H_{\text{kin}} = & -\frac{1}{4}t_0 \sum_{\{ij\}||ab,\sigma} \left\{ (3d_{ix\sigma}^\dagger d_{jx\sigma} + d_{iz\sigma}^\dagger d_{jz\sigma}) \pm \sqrt{3}(d_{ix\sigma}^\dagger d_{jz\sigma} \right. \\ & \left. + d_{iz\sigma}^\dagger d_{jx\sigma}) \right\} - t_0 \sum_{\{ij\}||c,\sigma} d_{iz\sigma}^\dagger d_{jz\sigma}. \end{aligned} \quad (3)$$

Here $d_{i\mu\sigma}^\dagger$ are creation operators for an electron in orbital $\mu = x, z$ with spin $\sigma = \uparrow, \downarrow$ at site i . The $\{i, j\}$ runs over pairs of nearest neighbours and gives two contributions for each bond $\langle i, j \rangle$; \pm is interpreted as plus sign for the bond $\langle i, j \rangle$ being parallel to the crystal axis a and minus for the bond $\langle i, j \rangle$ parallel to the axis b . (The crystallographic axis c is assumed to be aligned with Cartesian z -axis.)

The H_{int} and H_{spin} terms follow from the Coulomb interactions within a degenerate d band [34]; these terms are:

$$H_{\text{int}} = U_0 \sum_{i\mu} n_{i\mu\uparrow} n_{i\mu\downarrow} + (U_0 - \frac{5}{2}J_H) \sum_i n_{ix} n_{iz}, \quad (4)$$

$$H_{\text{spin}} = -\frac{1}{2}J_H \sum_i (n_{ix\uparrow} - n_{ix\downarrow})(n_{iz\uparrow} - n_{iz\downarrow}) \quad (5)$$

$$-J_H \sum_{i\mu} S_i^z (n_{i\mu\uparrow} - n_{i\mu\downarrow}) + \frac{1}{2}J' \sum_{\langle ij \rangle} S_i^z S_j^z, \quad (6)$$

$$(7)$$

Here H_{int} describes the charge interactions within the e_g subsystem and plays a role in doped manganites. The spin interactions H_{spin} include the leading part of Hund's exchange J_H , both between two e_g electrons at the same site, and between $s = 1/2$ spin of a single e_g electron and the $S = 3/2$ core t_{2g} spin at each site. On-site intraorbital Coulomb interaction is denoted as U_0 , and the interorbital Coulomb interaction is a linear combination of this term and Hund's exchange J_H [34]. Note that we include here only the leading Ising part of Hund's interaction terms, which is an approximation. However, within the present method using the correlated wave functions which are obtained by correcting the Hartree-Fock (HF) approximation, the remaining transverse terms do not contribute, compare refs. [32, 33]). The term $\propto J'$ is the antiferromagnetic (AF) superexchange generated by charge excitations of t_{2g} electrons, which lead to AF Heisenberg interaction between frozen core t_{2g} electrons [8, 12, 29]. This frozen-core approximation for $S = 3/2$ core spins works well for the description of the ground state properties as shown by earlier studies, see e.g. refs. [11, 35].

Finally, the Jahn-Teller H_{JT} part is [1, 7, 13, 36, 37]:

$$H_{\text{JT}} = \sum_i \left\{ g_{\text{JT}} \left(Q_{1i}(n_{ix} + n_{iz}) + Q_{2i}\tau_i^x + Q_{3i}\tau_i^z \right) \right. \quad (8)$$

$$\left. + \frac{K}{2}(2Q_{1i}^2 + Q_{2i}^2 + Q_{3i}^2) \right\}. \quad (9)$$

and includes three different Jahn-Teller modes $\{Q_{1i}, Q_{2i}, Q_{3i}\}$ at each site. The operators τ_i^α in H_{JT} are constructed for $\tau = 1/2$ orbital pseudospin for e_g electrons at site i [1, 8, 11–13],

$$\begin{aligned} \tau_i^x &\equiv \sum_{\sigma} (d_{ix\sigma}^\dagger d_{iz\sigma} + d_{iz\sigma}^\dagger d_{ix\sigma}), \\ \tau_i^z &\equiv \sum_{\sigma} (d_{ix\sigma}^\dagger d_{ix\sigma} - d_{iz\sigma}^\dagger d_{iz\sigma}), \end{aligned} \quad (10)$$

while Q_{1i} , Q_{2i} and Q_{3i} denote the active Jahn-Teller deformation modes of the i -th octahedron. (For simplicity the harmonic constant of the isotropic Jahn-Teller (breathing) mode Q_1 is assumed to be double with respect to those corresponding to Q_2 and Q_3 unsymmetric modes as discussed in ref. [1]). The breathing mode is quite often neglected in the effective models for the perovskite manganites, and plays no role in the undoped system. As we are dealing here with doped systems, we decided to keep it to investigate its consequences.

The crystal field splitting between z and x orbitals (2) was assumed to be zero (this approximation seems reasonable in quasi-cubic 3D manganites [13] though some authors [12] assume instead small finite values). Below we describe the numerical

simulations performed on finite 3D clusters with the above model (1). The variants of the described model reproduced the observed sequence of magnetic phases for increasing hole doping in 2D monolayer and bilayer manganites [32, 33].

2.2. Cluster approach including electron correlations

We studied $4 \times 4 \times 4$ clusters with periodic boundary conditions (PBC) filled by different number of e_g electrons, corresponding to the undoped LaMnO_3 system, and to systems with doping one-eighth ($x = 0.125$), quarter-doped system ($x = 0.25$) and half-doped system ($x = 0.5$). All calculations were performed at zero temperature ($T = 0$ K). First, the calculations within the single-determinant HF approximation were performed to determine the ground state wave function $|\Phi_0\rangle$. Also the energetic distance Δ between the highest occupied molecular orbital (HOMO) and the lowest unoccupied molecular orbital (LUMO) (HOMO-LUMO gap) was extracted at this step.

In the next step each HF wave function was independently modified to improve the energy and to include the electron correlations using the so-called local ansatz (for details see refs. [30–33]). We used the ansatz for the correlated ground state,

$$|\Psi\rangle = \exp\left(\sum_i \eta_i O_i\right) |\Phi_0\rangle, \quad (11)$$

where $\{\eta_i\}$ are variational parameters, and $\{O_i\}$ is a set of local correlation operators. These operators include the leading local density-density correlations in the present model for the perovskite manganites, in analogy to the 2D layered manganites, see refs. [32, 33]. These local operators used in the present model correspond to the subselection of the most important two electron excitations within the *ab initio* configuration–interaction method. The variational parameters $\{\eta_i\}$ were found by minimising the total energy

$$E_{\text{tot}} = \frac{\langle \Psi | H | \Psi \rangle}{\langle \Psi | \Psi \rangle}. \quad (12)$$

In this way the correlation energy,

$$E_{\text{corr}} = E_{\text{tot}} - E_{\text{HF}}, \quad (13)$$

was obtained.

Coming to technical details, in the first step HF computations were performed for each considered electron filling, starting from one of several different initial conditions (about a thousand for each set of Hamiltonian parameters), i.e., from predefined (some symmetric but mostly random) charge distribution, spin configuration, the latter selected from eight predefined patterns of core t_{2g} spins (see figure 1 of ref. [33]), and from several predefined sets of classical variables $\{Q_{1i}, Q_{2i}, Q_{3i}\}$. For each fixed set of the starting parameters and starting initial conditions on convergence we obtained a HF wave function which was a candidate for the ground state wave function. This self-consistent procedure was performed to provide energy minimum also with respect to the $\{Q_{1i}, Q_{2i}, Q_{3i}\}$ classical variables [32, 33].

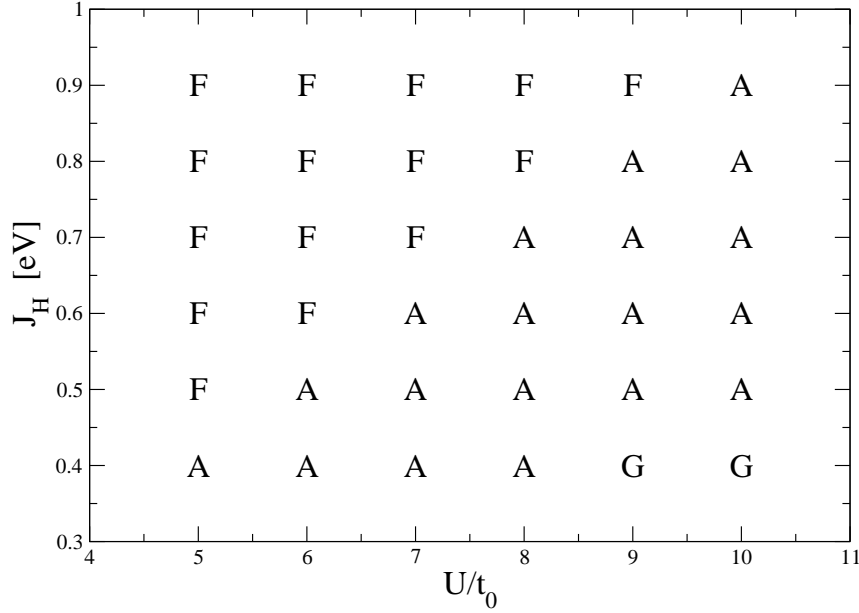


Figure 1. A simplified phase diagram in (U, J_H) plane for undoped ($x = 0$) LaMnO_3 . G refers to an ordinary Néel antiferromagnet (G -AF phase), A to A -AF phase with FM planes and AF coupling along the direction perpendicular to them, and F stands for the FM phase. Parameters: $t_0 = 0.4$ eV, $g_{\text{JT}} = 2.2$ eV \AA^{-1} , $K = 13$ eV \AA^{-2} and $J' = 3$ meV.

After completing the HF computations we performed correlation computations (as a second step for each investigated wave function) obtaining the total energy (12) and the correlation energy (13) (for more details see refs. [30–32]). After obtaining the total energy for one configuration, we repeated the entire procedure from the beginning, i.e., we took another (second) set of HF initial conditions and repeat all computations to obtain the second candidate for the ground state. Similarly for the third, fourth, \dots , *etcetera*, set of initial conditions. Finally, the resulting set of total energies was inspected and the lowest one was identified as a good candidate for the true ground state.

3. Numerical results

As the parameters of the model (1) are known only with certain accuracy, the computations were repeated for many sets of the Hamiltonian parameters. The values of the parameters which one should consider as realistic for $\text{La}_{1-x}(\text{Sr,Ca})_x\text{MnO}_3$ were extensively discussed in the literature (for a review in context of the present paper see refs. [1, 11, 32, 33]). Following the standard parameter sets [32, 33], we assumed that $t_0 = 0.4$ eV and the intraorbital Coulomb element is limited in the range $5 < U/t_0 < 12$. The values of Hund’s exchange are larger than t_0 [9, 29, 38], and we considered $t_0 < J_H < 2t_0$. The Jahn-Teller constant K was fixed as $K = 13$ eV \AA^{-2} [1, 2, 30, 32, 39]. Not much is known about the value of the coupling constant g_{JT} , therefore following discussion in ref. [1] we assumed that $2 \text{ eV } \text{\AA}^{-1} < g_{\text{JT}} < 3.7 \text{ eV } \text{\AA}^{-1}$.

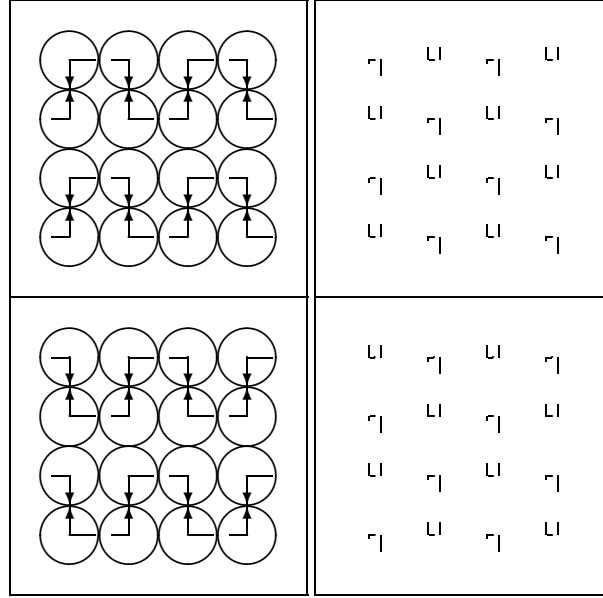


Figure 2. Charge distribution, magnetic, and orbital order of e_g electrons in the A-AF phase of LaMnO_3 , as obtained in undoped $4 \times 4 \times 4$ cluster with PBC. charge and alternating x, z orbital order for e_g electrons Only single ab planes are shown. Core t_{2g} spins are not shown. Left side panels — At each site the circle diameter corresponds to total e_g on-site charge; the arrow length to the e_g spin; the horizontal bar length to charge density difference between x and z orbitals (longest bar to the right corresponds to pure x , to the left to pure z , zero length to half by half combination). All these values are expressed in approximate proportionality (as generated by graphic package of latex) to nearest neighbour site-site distance which is assumed to be unity. Upper panels show situation on even numbered ab planes, lower panels correspond to odd numbered ab planes. Right side panels — Jahn-Teller distortions for the same even and odd ab planes: Q_{2i} (bars down slightly to the left of each site) and Q_{3i} (bars to the right of each site), and isotropic Q_1 (breathing) mode in between. For more clarity Q_2 and Q_3 bars are enlarged by factor of 2 compared to Q_1 . In the present case all Q_{1i} take the value of -0.08 \AA , the largest Q_{2i} is equal to 0.10 \AA , the largest Q_{3i} is 0.14 \AA .

And, finally, following recommendation of refs. [13, 29] we use the experimental value of the Néel temperature in CaMnO_3 [40], where e_g electrons are absent and the isotropic superexchange between core t_{2g} spins follows solely from the excitations of t_{2g} electrons, to fix $J' = 3 \text{ meV}$. Thus we have three fixed and three free parameters.

The aim was to identify the set (or sets) of these three free parameters which lead to good agreement of the model predictions with experimental data. This task turned out to be rather difficult especially with respect to Jahn-Teller parameter g_{JT} . Actually almost all values of g_{JT} either yield conducting state for both $x = 0.125$ and $x = 0.25$ doping levels, or they yield an insulator, also for both above doping levels. This contradicts the experimental situation as $\text{La}_{1-x}\text{Sr}_x\text{MnO}_3$ manganite is weakly insulating for $x = 0.125$ and conducting for $x = 0.250$ [41]. This insulator-to-metal transition turned out to be very useful as it allowed us to fix all three free parameters. The values

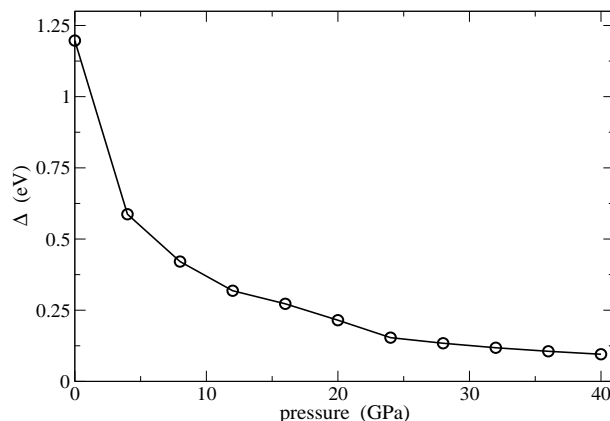


Figure 3. HOMO-LUMO gap Δ for increasing pressure p in the undoped LaMnO_3 : results of the calculations are shown by circles, solid line is a guide to the eye. The linear dependence of $t_0(p)$ and $K(p)$ on pressure is assumed. Other Hamiltonian parameters take standard values, see the caption of figure 2.

of the parameters which can bring out the agreement with the experimental data form a small isolated region within the parameter space, and finding them required making hundreds of scans through the parameter space. We have found that only for $U/t_0 = 8$, $J_H = 0.7$ eV and $g_{\text{JT}} = 2.2$ eV \AA^{-1} we are able to reproduce the experimental results.

3.1. Undoped LaMnO_3

The insulating phase in LaMnO_3 was reproduced by the present calculations. For the magnetic order we obtained robust A -AF structure, which has ferromagnetic (FM) order in ab planes, coupled by AF interaction in the c direction. This phase is almost generic and can be reproduced on the phase diagram for many sets of Hamiltonian parameters. Moreover, the correlation energy is small (see Table 1) and does not change the magnetic and orbital order obtained from the HF wave functions. To give an example, let us show one 2D section of our simplified phase diagram. Note that as long as we ignore the global structural distortion of the lattice below that structural phase transition, all cubic directions are equivalent and A -AF order shown in figure 1 applies also e.g. to FM order in ac planes accompanied by the AF coupling along the b direction.

As already mentioned the experimental data on conductivity fix the electron interaction parameters $U/t_0 = 8$ and $J_H = 0.7$ eV, as well as $g_{\text{JT}} = 2.2$ eV \AA^{-1} . For these parameters the ground state ordering for LaMnO_3 is shown in figure 2. The Jahn-Teller Q_2 and Q_3 distortions measured in ref. [23] (at $T = 200$ K) are only roughly in agreement with our results. (Note that for simplicity the cubic Jahn-Teller terms [7, 13] in H_{JT} were omitted. Therefore, the Jahn-Teller distortions we obtained are only estimations rather than the precise values).

We have found a large HOMO-LUMO gap Δ for LaMnO_3 which is an indicator that the obtained A -AF phase is insulating, see figure 3. It is known that at pressure of

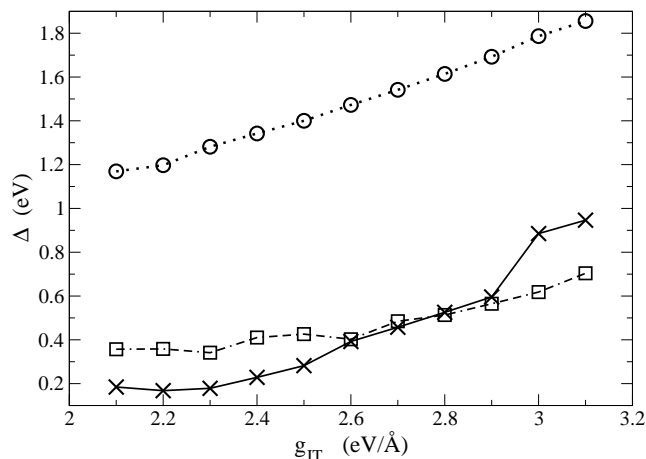


Figure 4. HOMO-LUMO gap Δ for increasing Jahn-Teller coupling g_{JT} . Circles, squares and crosses correspond to $x = 0$, $x = 0.125$ and $x = 0.25$, respectively. Parameters: $t_0 = 0.4$ eV, $U/t_0 = 8$, $J_H = 0.7$ eV, $J' = 3$ meV.

32 GPa LaMnO_3 becomes conducting [42]. In order to investigate the effect of pressure we followed heuristic argumentation presented in ref. [43] — it has been argued there (see figure 2 in ref. [43]) that the effect of 32 GPa pressure can be reproduced in a model similar to our effective model (1) when t_0 and K Hamiltonian parameters are renormalised in the following way: $t_0 \rightarrow 1.4t_0$ and $K \rightarrow 3.3K$. Following ref. [43], the other parameters (of the model) were left unchanged. We note that this assumption is somewhat unrealistic as at least the superexchange J' would also increase under pressure, but this effect is not important as long as we investigate the ground state and the magnetic structure does not change. U_0 and other effective parameters of the Hamiltonian should also show some limited variation under increasing pressure.

Inserting the new renormalised values of hopping and Jahn-Teller constant into our computations we found that the high pressure phase is indeed a conductor and we could identify the conducting phase as perfect charge-homogeneous, FM phase with zero Jahn-Teller distortions and with perfect half-to-half ($x^2 - y^2$) and ($3z^2 - r^2$) orbital order on each individual site. This orbital liquid state occurs in the doped FM manganites under normal pressure [44].

To provide a better evidence to such a prediction we plotted HOMO-LUMO gap Δ for increasing pressure. For simplicity it was assumed that $t_0(p)$ and $K(p)$, where p denotes pressure, vary linearly from t_0 and K at $p = 0$ to $1.4t_0$ and $3.3K$ at $p = 32$ GPa. Anyway, the transition from insulating to conducting phase can be deduced from figure 3 and it occurs around $p \approx 30$ GPa where the gap becomes small enough, $\Delta \simeq 0.1$ eV. Note that in the present finite cluster one finds always a gap between HOMO and LUMO, but we have estimated that $\Delta \simeq 0.1$ eV corresponds to a metallic ground state in the bulk. To close the discussion on LaMnO_3 under pressure let us mention ref. [45] where magnetic and orbital order under uniaxial strain (only JT modes were pressure-renormalised) was studied by using similar (to our) Hamiltonian.

Table 1. Hartree-Fock energies E_{tot} and total ground state energies E_{HF} (12), both in eV, as obtained for $4 \times 4 \times 4$ cluster versus the doping x . Parameters of the Hamiltonian: $t_0 = 0.4$ eV, $U = 8t_0$, $J_H = 0.7$ eV, $K = 13$ eV/Å², $g = 2.2$ eV/Å, $J' = 3.0$ meV.

x	E_{HF}	E_{tot}
0.000	-96.016	-96.114
0.125	-88.217	-88.315
0.250	-79.374	-79.521
0.500	-58.666	-58.896

3.2. One-eight-doped $\text{La}_{0.875}\text{Sr}_{0.125}\text{MnO}_3$

In one-eight doped manganite one finds an insulating phase with FM order, both in the HF and for the correlated wave functions. The correlation energy is small, see Table 1, and does not change the magnetic and charge order in the system. The breathing mode Jahn-Teller distortions are small and uniform, $Q_{1i} \approx -0.08$ Å. This phase is characterized by a rather interesting charge and orbital distribution, with a distinct alternation in charge density between even and odd planes. Consequently, this phase is an insulator, in agreement with the experiment [41], though a weak one as indicated by rather small HOMO-LUMO gap shown in figure 4 (curve in the middle, squares). Note that gap is reduced by a factor close to 3 from the value obtained for LaMnO_3 .

The alternation of e_g electron density occurs between even and odd planes. First, in even numbered planes there are somewhat less electrons and the orbitals are of $(x^2 - y^2)$ character, $Q_{2i} \approx 0$ and Q_{3i} take the value of -0.1 Å. These distortions favor the x orbitals. However, there are also some exceptions, i.e., occasionally on a site we find the $(3z^2 - r^2)$ orbital occupied and $Q_{3i} \approx +0.1$ Å. The charges are distributed in a slightly non-homogeneous way, with the site to site variations of charge being at most $0.2 e$. Second, in the odd numbered planes one finds a little bigger average charge density per site than in the even planes and almost homogeneous charge distribution. In contrast to the even planes, one finds predominantly $(3z^2 - r^2)$ orbitals occupied. The Jahn-Teller distortions are $Q_{3i} \approx \pm 0.1$ Å and $Q_{2i} \approx \pm 0.1$ Å. Again, we have seen also some exceptions, with x orbitals occupied at a few sites and the corresponding modified Jahn-Teller distortions, similar to those in the even planes. In fact, this result shows that sites with differently occupied orbitals can proliferate between the even and odd planes and form charge and orbital defects in each plane. This shows that the inhomogeneous charge distribution is a generic feature in this range of doping.

3.3. Quarter-doped $\text{La}_{0.75}\text{Sr}_{0.25}\text{MnO}_3$

Also for quarter-doped manganites, such as $\text{La}_{0.75}\text{Sr}_{0.25}\text{MnO}_3$, one finds FM order and weakly non-homogeneous charge distribution with the present parameters (see figure 5). These results are similar to the ground state found for $x = 0.125$ — we have found again nonequivalent alternating planes, as described below. The correlations do not change this result, and are again weak (Table 1) as the local moments have formed and the

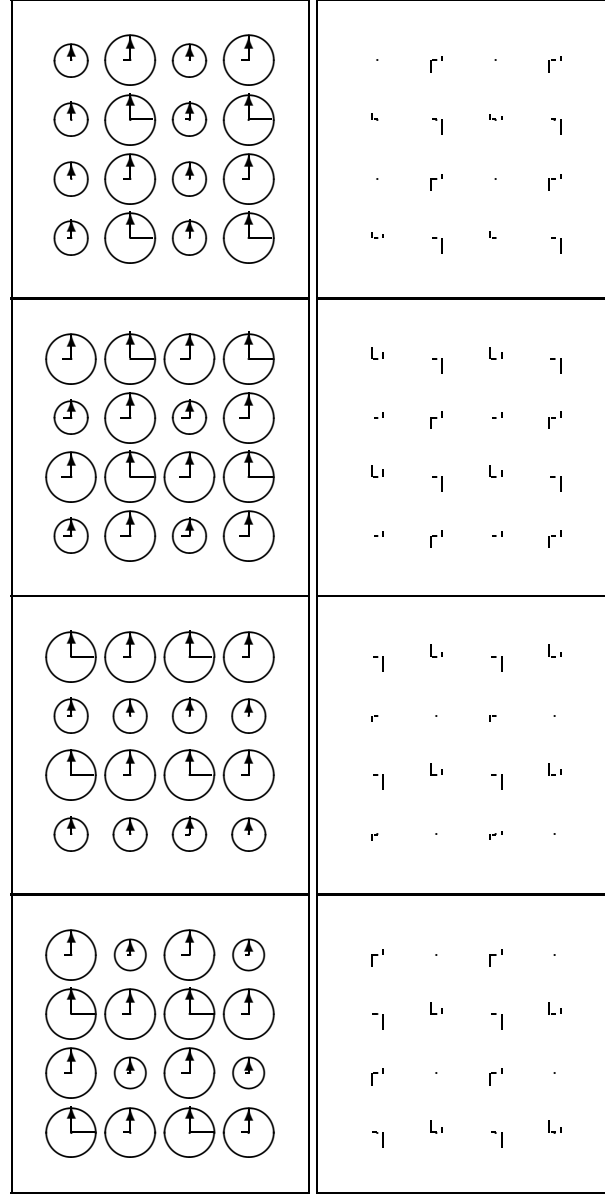


Figure 5. Magnetic A-AF, charge and orbital electron density for e_g electrons as obtained in quarter-doped manganites, $x = 0.25$. Four single ab planes (perpendicular to the c axis) extracted from $4 \times 4 \times 4$ cluster are shown. Core t_{2g} spins are not shown; their directions agree with the directions of e_g spins. The meaning of symbols and parameters are the same as in figure 2.

main effects are already captured in the HF approach.

On the one hand, within even numbered planes in the ground state one has weak charge order in form of a stripe phase, with vertical or horizontal charge-minority lines alternating with charge-majority lines (charge difference of about $0.2e$). Charge minority sites have mixed half to half x and z orbital occupancy and negligible Jahn-Teller distortions, which is characteristic for the orbital liquid in the metallic state [44]. The situation is quite different along the charge majority lines — one finds there half of these

sites with x orbitals and with negligible $\{Q_{1i}, Q_{2i}\}$ distortions, and with $Q_{3i} \approx -0.13$ Å. The other half of these sites carries the mixture of z and x roughly in proportion 2:1 and negligible $\{Q_{1i}, Q_{3i}\}$ distortions, whereas $Q_{2i} \approx -0.1$ Å. These sites with higher electron density (i.e., those with x orbitals and those with 2:1 orbitals z and x) alternate along the charge-majority lines.

On the other hand, on odd numbered planes the orbitals and Jahn-Teller distortions are much the same as the ones on even numbered planes (as described above). However there is a difference — along charge-minority lines (each second line in the cluster) we did not find homogeneous charge density but, instead alternating charge-minority and charge-majority sites.

The FM phase at $x = 0.25$ doping should be a metal which follows from quite small HOMO-LUMO gap ($\Delta \simeq 0.1$ eV), see figure 4. This result agrees with the phase diagram for the perovskite manganites [1, 46].

3.4. Half-doped $\text{La}_{0.5}\text{Sr}_{0.5}\text{MnO}_3$ — stability of the CE phase

Surprisingly, for half-doped $\text{La}_{0.5}\text{Sr}_{0.5}\text{MnO}_3$ one finds again almost the same ground state as for $x = 0.25$, namely FM spin order, accompanied by weakly non-homogeneous charge distribution and a conducting phase (HOMO-LUMO gap is about 0.12 eV). The ratio of x to z orbitals on each site is half to half, while the Jahn-Teller distortions are very small. These findings reproduce the experimental situation in $\text{La}_{0.5}\text{Sr}_{0.5}\text{MnO}_3$, where no CE phase was observed.

On the contrary, the CE phase was found in half-doped $\text{La}_{0.5}\text{Ca}_{0.5}\text{MnO}_3$ [47, 48]. A somewhat unprecise but still common point of view is that a manganite doped with strontium is more metallic than the manganite doped with calcium (more insulating) which in turn might be attributed to weaker coupling to the lattice by the Jahn-Teller interactions in strontium compounds and a bigger role of these interactions in calcium compounds. Indeed, the FM phase was found insulating in a broader range of doping in $\text{La}_{1-x}\text{Ca}_x\text{MnO}_3$ than in $\text{La}_{1-x}\text{Sr}_x\text{MnO}_3$ [49]. If this is the case then our effective model should provide a different prediction for the ground state when g_{JT} is larger.

When we discussed the precise values of Hamiltonian parameters following the discussion presented in ref. [1] we assumed $2 \text{ eV } \text{Å}^{-1} < g_{\text{JT}} < 3.7 \text{ eV } \text{Å}^{-1}$. Then for strontium manganite $\text{La}_{1-x}\text{Sr}_x\text{MnO}_3$ we found that $g_{\text{JT}} = 2.2 \text{ eV } \text{Å}^{-1}$. Now for the sake of the ongoing discussion for calcium doped manganite we will accept $g_{\text{JT}} = 3.7 \text{ eV } \text{Å}^{-1}$, the biggest value which is allowed. This change of the unique parameter immediately provides us with the expected result. Now the spin order in the ground state is indeed in form of FM zig-zags with AF order between them, characteristic for the CE phase, and the charge order is of checkerboard type (figure 6). The CE phase is quite robust, it is identified at the HF level and the correlations when added do not change this result. This is in contrast to what happens in bilayer half-doped manganites where the correlations stabilize the CE phase [33]. We note, however, that the magnetic moments are larger in the 3D system, and therefore the role of electron correlations in the magnetic states

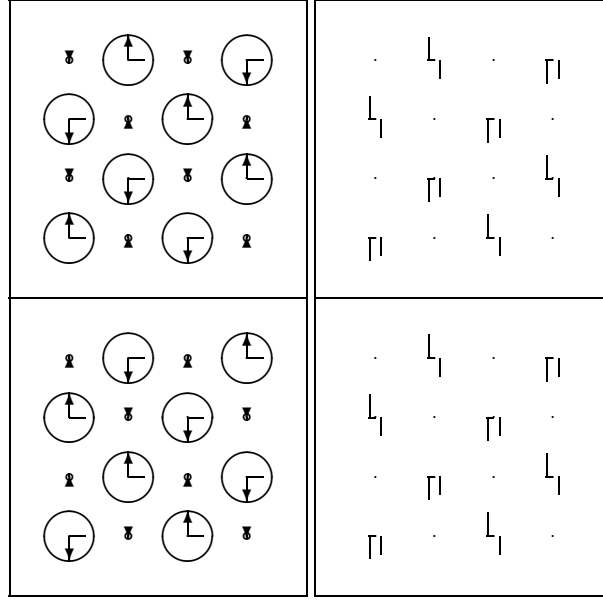


Figure 6. Magnetic CE, the ordered charges and fractions of occupied x and z orbitals for e_g electrons in half-doped $\text{La}_{0.5}\text{Ca}_{0.5}\text{MnO}_3$. The standard Hamiltonian parameters (which apply to strontium-doped substance) were assumed as in the caption of figure 2 with one exception, namely we adopted a larger Jahn-Teller coupling $g_{\text{JT}} = 3.7 \text{ eV } \text{\AA}^{-1}$. Two panels correspond to two neighboring nonequivalent ab planes — the order found in these planes is repeated along the c axis in the planes number 3 and 4, not shown. Only e_g spins are shown (T_{2g} spins are parallel to them at all sites). Note that the magnetic CE zig-zag-like order refers to the total spin thus it is not properly visible on the figure where only e_g spins are plotted. The legend is the same as in figure 2.

such as the CE phase is reduced.

3.5. Switching off Jahn-Teller distortions

The results presented up to now indicate the importance of Jahn-Teller interactions. Due to them local distortions are created at each doping level, and they influence both the electronic structure and the magnetic properties. It seems that the value of g_{JT} coupling is the primary factor which determines whether the 3D perovskite system is a conductor or an insulator. Therefore it seems reasonable to perform additional test computations switching off the Jahn-Teller interactions.

We performed such computation for $\text{La}_{1-x}\text{Sr}_x\text{MnO}_3$ where $x = 0, 0.125, 0.250$ and $g_{\text{JT}} = 0$. The resulting ground states were all the same: FM, charge homogeneous orbital liquid phase [44], with half to half ratio of x to z orbitals at each site and conducting (HOMO-LUMO gaps we found were all about 0.1 eV). This confirms the above point of view that the Jahn-Teller distortions play a crucial role for the charge, magnetic and orbital order in doped perovskite manganites.

4. General conclusions and final remarks

We considered the effective Hamiltonian for e_g electrons which takes into account their kinetic energy with anisotropic phase dependent hopping $\propto t$, on-site Coulomb interaction U , Hund's exchange coupling J_H , their coupling to frozen core t_{2g} electrons $\propto J_H$, the Heisenberg AF superexchange $\propto J'$ between core T_{2g} spins, and the Jahn-Teller interactions with lattice distortions. Due to the complexity of the problem, we could not provide a precise proof that this model is sufficient for the physical properties of the perovskite manganites, but rather we report on results of computations which demonstrate that all these interactions enter on equal footing and seem to be essential for correct interpretation of the experimental data. Indeed, we have performed also calculations with several sets ignoring one or the other interaction term, and the results were very unsatisfactory in all cases, i.e., such simplified models were not able to reproduce the experimental observations.

We would like to emphasize that the realistic Jahn-Teller coupling plays a rather special and a very important role in the manganites as it controls the conductivity of the perovskite 3D systems. We have presented evidence that this interaction generates local distortions in the entire investigated range of hole doping $0.125 \leq x \leq 0.50$ which lead to charge inhomogeneities, defects in the orbital occupancy, and influences the magnetic order. Such states have been seen before in the experimental data on doped manganites [50] and were also suggested to follow from the theoretical models [51]. Unfortunately, reliable studies of systems with charge disorder and local distortions are very difficult to perform, but the present results demonstrate that these states might decide about the colossal magnetoresistance and select one or the other type of magnetic order. Particularly at half-doping ($x = 0.5$) we have found a subtle balance between the FM phase and the CE phase, the latter stabilized by large Jahn-Teller interactions. This is not surprising as the nearest neighbor JT coupling might not be sufficient to stabilize the observed zigzag FM chains in the CE phase for the realistic parameters. The mechanism invoked in [52] to stabilize the CE phase is subtle and employs the cooperative JT interaction between next-nearest Mn^{3+} neighbors mediated by the breathing mode distortion of Mn^{4+} octahedra and displacements of Mn^{4+} ions.

As found before for monolayer and bilayer doped manganites, see refs. [30, 32], we have obtained many metastable ground states in the 3D system which are possible in principle. Such states are not discussed in detail in the present paper, but we just point out that they represent local energy minima and could be also realized at finite temperature. Therefore, the search for the best candidate for the true ground state requires examination of numerous phases with different kinds of nonhomogeneous charge distribution. Therefore, we suggest as a general conclusion that nonhomogeneous charge distribution is a generic feature of the doped perovskite manganites. It follows that the theoretical predictions which are based on models assuming just a few *a priori* selected candidates for the ground state (especially the ones with high symmetry of charge or orbital order) can not be fully conclusive unless they are based on reliable experimental

data.

Acknowledgments

We acknowledge financial support by the Polish Ministry of Science and Higher Education under Project No. N202 068 32/1481. A M Oleś was also supported by the Foundation for Polish Science (FNP).

References

- [1] Dagotto E, Hotta T and Moreo A 2001 *Physics Reports* **344** 1
Dagotto E 2005 *New J. Phys.* **7** 67
- [2] Millis A J 1996 *Phys. Rev. B* **53** 8434
Millis A J 1997 *Phys. Rev. B* **55** 6405
- [3] Saitoh T, Bocquet A E, Mizokawa T, Namatame H, Fujimori A, Abbate M, Takeda Y and Takano M 1995 *Phys. Rev. B* **51** 13942
- [4] Mizokawa T and Fujimori A 1996 *Phys. Rev. B* **54** 5368
Mizokawa T and Fujimori A 1997 *Phys. Rev. B* **56** R493
- [5] Benedetti P and Zeyher R 1999 *Phys. Rev. B* **59** 9923
Held K and Vollhardt D 2000 *Phys. Rev. Lett.* **84** 516
- [6] Taek Park K 2001 *J. Phys: Condens. Matter* **13** 9231
- [7] Popovic Z and Satpathy S 2000 *Phys. Rev. Lett.* **84** 1603
- [8] Hotta T, Malvezzi A L and Dagotto E 2000 *Phys. Rev. B* **62**, 9432
- [9] Kovaleva N N, Boris A V, Bernhard C, Kulakov A, Pimenov A, Balbashov A M, Khaliullin G and Keimer B 2004 *Phys. Rev. Lett.* **93** 147204
Kovaleva N N, Oleś A M, Balbashov A M, Maljuk A, Argyriou D N, Khaliullin G and Keimer B 2010 *Phys. Rev. B* **81** 235130
- [10] Ebata K, Mizokawa T and Fujimori A 2005 *Phys. Rev. B* **72** 233104
- [11] Daghofer M, Oleś A M and von der Linden W 2004 *Phys. Rev. B* **70** 184430
Daghofer M, Oleś A M, Nauber D and von der Linden W 2006 *Phys. Rev. B* **73** 104451
Daghofer M and Oleś A M 2007 *Acta Phys. Polon. A* **111** 497
- [12] Wei-Guo Yin, Volja D and Wei Ku 2006 *Phys. Rev. Lett.* **96** 116405
- [13] Lin C and Millis A J 2008 *Phys. Rev. B* **78** 174419
- [14] Maezono R, Ishihara S and Nagaosa N 1998 *Phys. Rev. B* **58** 11583
- [15] Moritomo Y, Arima T and Tokura Y 1995 *J. Phys. Soc. Japan* **64** 4177
- [16] Morimoto Y, Tomioka Y, Asamitsu A and Tokura Y 1995 *Phys. Rev. B* **51** 3297
- [17] Sternlieb B J, Hill J P, Wildgruber U C, Luke G M, Nachumi B, Morimoto Y and Tokura Y 1996 *Phys. Rev. Lett.* **76** 2169
- [18] Park J H, Chen C T, Cheong S-W, Bao W, Meigs G, Chakarian V, and Idzerda Y U 1996 *Phys. Rev. Lett.* **76** 4215
- [19] Jung J H, Ahn J S, Yu J, and Noh T W, Lee J, Moritomo Y, Solovyev I and Terakura K 2000 *Phys. Rev. B* **61** 6902
- [20] Perring T G, Adroja D T, Caboussant G, Aeppli C, Kimura T and Tokura Y 2001 *Phys. Rev. Lett.* **87** 217201
- [21] Wilkins S B, Spencer P D, Hatton P D, Collins S P, Roper M D, Prabhakaran D and Boothroyd A T 2003 *Phys. Rev. Lett.* **91** 167205
- [22] Wilkins S B, Stojić N, Beale T A W, Binggeli N, Hatton P D, Bencok P, Stanescu S, Mitchell J F, Abbamonte P and Altarelli M 2006 *J. Phys.: Condensed Matter* **18** L323
- [23] Chatterji T, Fauth F, Ouladdiaf B, Mandal P, and Ghosh B 2003 *Phys. Rev. B* **68** 052406

- [24] Huang D J, Wu W B, Guo G Y, Lin H-J, Hou T Y, Chang C F, Chen C T, Fujimori A, Kimura T, Huang H B, Tanaka A and T. Jo T 2004 *Phys. Rev. Lett.* **92** 087202
- [25] Senff D, Reutler P, Braden M, Friedt O, Bruns D, Cousson A, Bourée F, Merz M, Büchner B and Revcolevschi A 2005 *Phys. Rev. B* **71** 024425
- [26] Larochelle S, Mehta A, Lu L, Mang P K, Vajk O P, Kaneko N, Lynn J W, Zhou L and Greven M 2005 *Phys. Rev. B* **71** 024435
- [27] Oleś A M 2010 *Acta Phys. Polon. A* **118** 212
- [28] Yamasaki A, Feldbacher M, Yang Y-F, Andersen O K and Held K 2006 *Phys. Rev. Lett.* **96** 166401
- [29] Feiner L F and Oleś A M 1999 *Phys. Rev. B* **59** 3295
- [30] Rościszewski K and Oleś A M 2003 *J. Phys.: Condensed Matter* **15** 8363
- [31] Rościszewski K and Oleś A M 2005 *Phys. Stat. Sol. (b)* **243**, 155
- [32] Rościszewski K and Oleś A M 2007 *J. Phys.: Condensed Matter* **19** 186223
- [33] Rościszewski K and Oleś A M 2008 *J. Phys.: Condensed Matter* **20** 365212
- [34] Oleś A M 1983 *Phys. Rev. B* **28** 327
- [35] Weisse A and Feshke H 2004 *New J. Phys.* **6** 158
- [36] J. Bała J and Oleś A M 2000 *Phys. Rev. B* **62** R6085
- [37] Salafranca J and Brey L 2006 *Phys. Rev. B* **73** 024422
- [38] Oleś A M and Feiner L F 2002 *Phys. Rev. B* **65** 052414
- [39] Bała J, Oleś A M and Sawatzky G A 2002 *Phys. Rev. B* **65** 184414
- [40] Nicastrro M and Patterson C H 2002 *Phys. Rev. B* **65** 205111
- [41] Urushibara A, Moritomo Y, Arima T, Asamitsu A, Kido G and Tokura Y 1995 *Phys. Rev. B* **51** 14103
- [42] Loa I, Adler P, Grzechnik A, Syassen K, Schwarz U, Hanfland M, Rosenberg G K, Gorodetsky P and Pasternak M P 2001 *Phys. Rev. Lett.* **87** 125501
- [43] Fuhr J F, Avignon M and Alascio B 2008 *Phys. Rev. Lett.* **100** 216402
- [44] Feiner L F and Oleś A M 2005 *Phys. Rev. B* **71** 144422
- [45] Nanda B R K and Satpathy S 2010 *Phys. Rev. B* **81** 174423
- [46] Schiffer P, Ramirez A P, Bao W and Cheong S-W 1995 *Phys. Rev. Lett.* **75** 3336
- [47] Wollan E O and Koehler W C 1955 *Phys. Rev.* **100** 545
- [48] Radelli P G, Cox D E, Marezio M and Cheong S-W 1997 *Phys. Rev. B* **55** 3015
- [49] Moussa F, Hennion M, Kober-Lehouelleur P, Reznik D, Petit S, Moudden H, Ivanov A, Mukovskii Y A, Privezentsev R and Albenque-Rullier F 2007 *Phys. Rev. B* **76** 064403
- [50] Louca D, Egami T, Brosha E L, Röder H and Bishop A R 1997 *Phys. Rev. B* **56** R8475
Louca D and Egami T 1999 *Phys. Rev. B* **59** 6193
- [51] Aliaga H, Normand B, Hallberg K, Avignon M and Alascio B 2001 *Phys. Rev. B* **64** 024422
Alvarez G, Aliaga H, Şen C and Dagotto E 2006 *Phys. Rev. B* **73** 224426
- [52] Bała J, Horsch P and F. Mack F 2004 *Phys. Rev. B* **69** 094415
Bała J, and Horsch P 2005 *Phys. Rev. B* **72** 012404